Nonintrusive Optical Visualization of Surface Nanobubbles

Stefan Karpitschka,[1,*] Erik Dietrich,[2,3,†] James R. T. Seddon,[2,‡] Harold J. W. Zandvliet,[3,§] Detlef Lohse,[2,‖] and Hans Riegler[1,¶]

[1]*Department of Interfaces, Max Planck Institute of Colloids and Interfaces, Research Campus Potsdam-Golm, 14476 Potsdam, Germany*

[2]*Physics of Fluids, MESA+ Institute for Nanotechnology, University of Twente, P.O. Box 217, 7500 AE Enschede, The Netherlands*

[3]*Physics of Interfaces and Nanomaterials, MESA+ Institute for Nanotechnology, University of Twente, P.O. Box 217, 7500 AE Enschede, The Netherlands*

(Received 16 April 2012; revised manuscript received 18 June 2012; published 9 August 2012)

Individual surface nanobubbles are visualized with nonintrusive optical interference-enhanced reflection microscopy, demonstrating that their formation is not a consequence of the hitherto used intrusive atomic force microscopy technique. We then use this new and fast technique to demonstrate that surface nanobubbles form in less than a few seconds after ethanol-water exchange, which is the standard procedure for their preparation, and examine how they react to temperature variations.

DOI: 10.1103/PhysRevLett.109.066102 PACS numbers: 68.08.−p

Surface nanobubbles are nanoscopic gaseous objects on immersed substrates, which can survive for days, in contrast with classical expectation [1,2]. The existence of surface nanobubbles can be inferred from attenuated total reflection infrared spectroscopy [3], quartz crystal microbalance [4,5], neutron reflectometry [6,7], and x-ray reflectivity [8]. All of these techniques provide a single number that describes the thickness of a gassy layer at the immersed near-wall region, typically a spatial average of many hundred square microns. This is much larger than the 10^{-2} μm^2 footprint area of an individual surface nanobubble. Therefore, the results of these techniques may also be (and often are) interpreted as a uniform gassy layer trapped between substrate and liquid.

Up to now, individual nanobubbles have been imaged only through atomic force microscopy (AFM) [9,10], whereby an immersed nanometric probe is rapidly tapped against a solid surface. In fact, AFM is currently the main tool for their investigation, and the visualization of the nanobubbles has finally convinced many critics, who questioned their existence as inferred from the nonimaging, area-averaging methods mentioned above. Nevertheless, AFM imaging is intrusive and rather slow (as compared to optical methods), and so there are still plenty of open questions. Bringing in a rapidly vibrating nanoscopic probe could actually lead to the breakdown of a uniform gassy layer into nanobubbles, as the negative pressure divergence during each retraction (often at $\sim 10^4$ Hz) may cause nucleation. So, do we see surface nanobubbles with the AFM because of the intrusive measurement technique? Does the intrusive and potentially nucleation-promoting impact induce a random nucleation? Do preferential nucleation sites dominate bubble formation if there is no external intrusive stimulus; i.e., do bubbles in this case always appear at the same location? How fast do the nanobubbles appear (grow) without external intrusion after providing suitable growth conditions, e.g., through ethanol-water exchange?

In this Letter, we propose to address and answer these questions by using a new technique to investigate nanobubbles, namely, optical interference-enhanced reflection microscopy [11]. This technique is nonintrusive and much faster than AFM. In the first part of this Letter, we will establish that we observe the same objects with this new technique as we do with the standard AFM technique. In the second part of the Letter, we will employ the technique to study the dynamics and temperature dependence of surface nanobubbles on the fast time scale of seconds, which is inaccessible with AFM. Our method is complementary to the total internal reflection fluorescence technique, which was recently employed for nanobubble visualization [12]. In that study, the nanobubbles were visualized from the bottom, and the contrast was enhanced through the addition of rhodamine.

Imaging technique and substrate surface preparation.—Optical interference-enhanced reflection microscopy uses a planar, suitably layered surface to increase the reflected intensity contrast between bare surface areas and regions covered by thin transparent objects. As a layer for interference enhancement, we use an artificially grown oxide (silica) layer of 300 nm on silicon wafers (Silchem, Freiberg, Germany). In this case, light from an incident water-immersed microscope objective hits areas without interfacial objects, and passes through the water, the substrate coating, and the oxide layer (Fig. 1). At each interface, a certain amount of light is reflected back (mainly at the silicon–silicon-oxide interface), resulting in reflected intensity from the interference of the beams. A transparent object at the air-substrate interface, such as a nanobubble, changes the reflectivity due to the additional interfaces. The reflectivity contrast between the interface sections with and without attached bubbles is maximized by (empirically) selecting an optimum wavelength. For laterally small and/or nonplanar interfacial objects, the observed

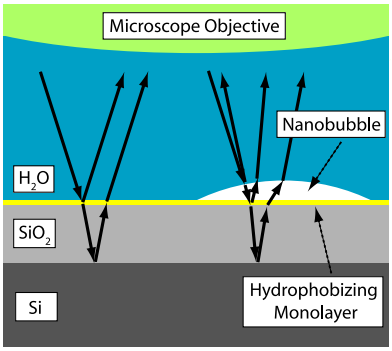

FIG. 1 (color online). Schematic diagram of the optical interference-enhanced reflection microscopy technique. The locally reflected light intensity is the sum of the reflected beams. It is different for surfaces with and without adsorbed transparent objects (e.g., nanobubbles). An appropriate thickness of the SiO_2 layer (300 nm thick) and a suitable wavelength significantly enhance the contrast. Because the footprint diameter of the nanobubbles is usually smaller than the wavelength, they also act as scattering objects (corresponding light paths not shown in the figure). Thus, the imaging does not necessarily show the geometry of the nanobubbles, and the nanobubbles typically appear as dark spots, as the scattered light is lost for the imaging.

intensity from the interface results from reflection as well as diffraction or scattering contributions. Therefore, the resulting microscopy images have to be analyzed very carefully for quantitative statements. Nonetheless, this technique allows for the visualization of transparent objects that are thinner than nanometers [11].

The contrast was further amplified by online image processing, such as oversampling and background subtraction, for which images were taken from the substrate surface without nanobubbles, i.e., immersed in degassed (Millipore) water. The purpose of the background subtraction is the reduction of device-specific imaging artifacts, such as illumination heterogeneities. Background images were also taken from surface regions with persisting small artifacts (scratches, dust particles) in a characteristic arrangement. These artifacts assure proper focusing on the otherwise featureless interface plane. In addition, they serve as position markers, allowing for the unambiguous identification or recognition of particular surface regions.

To enhance nanobubble formation, the silicon substrates were hydrophobized through vapor deposition [13] of perfluorodecyldimethylchlorosilane (PFDDMCS) [14]. Interfacial nanobubbles were created by the currently established protocol of ethanol-water exchange [15]. To this end, the degassed water was first replaced with ethanol (analysis grade, 99.9%). Then, the ethanol was replaced again by water that was supersaturated with gas (bubbling with N_2 at 4 °C for 30 min). This step of ethanol-water exchange reliably leads to the formation of interfacial nanobubbles [10,16]. The volume of the immersion drop on the substrate was ≈ 100 μL. The flow rate was typically 10 μL/s. To ensure complete liquid replacement, the

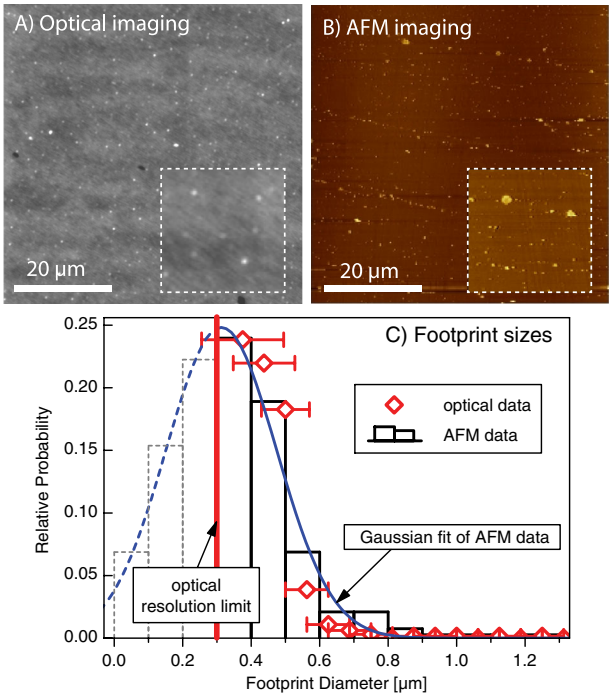

FIG. 2 (color online). Comparison between the imaging of surface nanobubbles by (a) interference-enhanced reflection microscopy and (b) AFM. Identically prepared samples were imaged under the same conditions (same surface preparation and same liquid exchange protocol, but the images do not show identical surface areas). Inserts are 10 μm $\times$ 10 μm zooms of the images. The AFM measurements were performed with an Agilent 5100 [tapping mode with 4.5 N/m, 10 nm noncontact silicon conical probes (MikroMasch), and dry resonance 150 kHz]. The height range in the AFM images is 40 nm. (c) Distribution of nanobubble footprint diameters measured with both techniques. Optically, only diameters above 300 nm [$\lambda/(2 \times$ numerical aperture)] can safely be quantified. Within these limitations, the size distributions are in good agreement.

exchange volume was 1 mL; i.e., liquid exchange was performed for 100 s. The imaging process itself (focusing, oversampling) has a time resolution of $\sim$1 s.

Comparison between optical imaging and AFM.—A typical image of the PFDDMCS surface after nanobubble nucleation is shown in Fig. 2(a). The corresponding AFM image of the identically treated surface [Fig. 2(b)] of course contains many more surface nanobubbles than the optical image, namely, the ones below the optical resolution, but it is also clear that the AFM image contains several larger nanobubbles consistent with those seen in the optical image. Thus, the circular features detected with our optical technique appear similar to those measured with AFM. To further support that the optically observed features are indeed surface nanobubbles, we plot their relative size distributions in Fig. 2(c) for both techniques. The AFM-measured nanobubble size distribution is Gaussian, as shown by the blue fit, with a peak corresponding to a footprint diameter of 350 nm, in agreement with

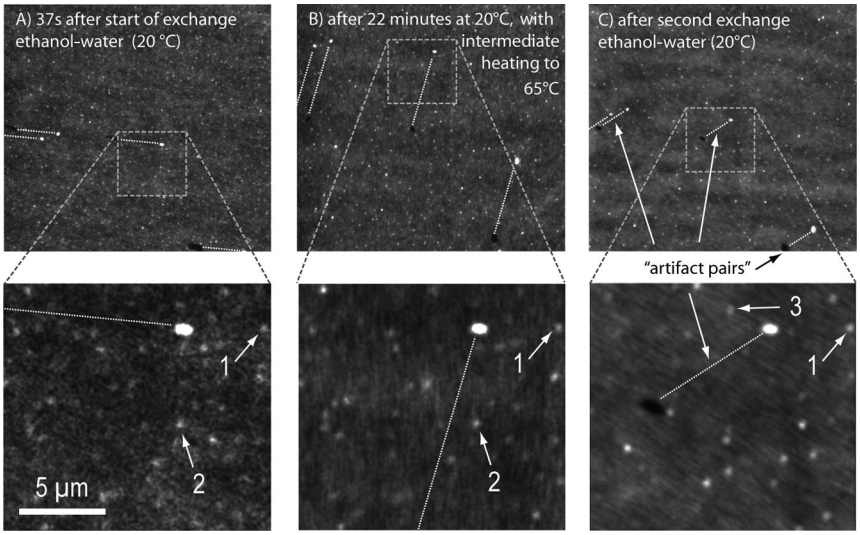

FIG. 3. Interference-enhanced optical microscopy images of a hydrophobic interface wetted by water (super)saturated with N_2 after ethanol-water exchange. The bright dots originate from nanobubbles. These act as scattering objects, and in the original imaging they appear as darker spots compared to the reflecting bare surface; for better visibility here, we inverted the contrast. The nanobubbles are only visible after the ethanol-water exchange. Background images without nanobubbles, which were used for background subtraction (for contrast enhancement), are featureless except for surface artifacts (scratches, dust particles). The three frames show the surface after various times or treatments as indicated (see the main text). The images of the top row show roughly the same surface region. The magnified sections show the exact same surface regions for all the three cases. This is possible thanks to the dark or bright ''artifact pairs'' that originate from persistent surface artifacts and serve as position markers. The different relative orientation or distance of the dark or bright artifact spots results from the different relative positions of the sample in each experiment as well as the background recording. For the description of the specifically numbered nanobubbles (1, 2, and 3), we refer to the main text.

previous statistical measures for nanobubbles [17,18]. The size distribution of the optically measured dark spots is also plotted in Fig. 2(c), shown as the red diamonds on top of the AFM histogram and Gaussian fit. [Note that the images in Figs. 2(a) and 3 are inverted for better visibility.] The optical distribution fits well with the AFM distribution [19]. Thus, the objects observed with our optical technique seem to be comparable in size and size distribution to the surface nanobubbles measured using AFM. Further comparisons between the results obtained with the two techniques are presented in the Supplemental Material [20].

Nanobubble dynamics, locations, and temperature dependence.—We now employ interference-enhanced imaging of surface nanobubbles to further explore the nanobubbles on a fast time scale. The images in Fig. 3(a) were recorded right after the ethanol-water exchange; the images in Fig. 3(b) were recorded after some time, with a heating cycle in between; and the images in Fig. 3(c) were recorded after a second round of ethanol-water exchange. In all cases, the images reveal bright dots, which originate from nanobubbles. This can be concluded from the correlation between the appearance of the dots and the sample treatment. The bright spots are visible only after the ethanol-water exchange.

The background images were taken under the same imaging conditions from the same sample surface region wetted by (degassed) water without prior ethanol-water exchange. As mentioned earlier, these interfaces are nanobubble-free and, in fact, do not show any of the small bright spots (only the bright spots from the persisting artifacts). This is unambiguously clear from the images with the bright spots or nanobubbles presented in Fig. 3. If the background images contained similar bright spots, these would show up as dark spots in the background-subtracted images. This is not the case. Only the persisting artifacts do show up as bright or dark ''artifact pairs.'' This proves that the interface was indeed in focus in both cases, and poor focusing or imaging is not the reason why the nanobubble-free interface does not show bright spots. The relative arrangement of the artifact pairs helps to find the same sample surface region after the various treatments, and therefore an identical, magnified section can be identified and is presented in the three frames of the second row.

Nanobubbles appear very rapidly after the liquid exchange, as shown in Fig. 3(a). The image was taken 37 s after the start of the liquid exchange. The complete exchange of the liquid volume of the light path under the objective lens took approximately 30 s; i.e., after 30 s the ethanol was replaced by water. This can be inferred directly from the imaging: up to about 30 s after the start of the liquid exchange, it was not possible to focus on the interface because of spatiotemporal variations of the refractive index, i.e., variations of the liquid composition. As soon as focusing or imaging was possible, the bright dots were visible. This means that the nanobubbles appear and

fully develop within seconds or faster after the replacement of the ethanol by water.

The second image, Fig. 3(b), is of the same surface region after 22 min and an intermediate heating cycle. The sample was kept for 7 min at 20 °C, then heated within 7 min to 65 °C and again cooled to 20 °C within 7 min. Then, the image was recorded. A comparison between the images taken straight after finishing the liquid exchange at 20 °C [Fig. 3(a)] and 22 min later with the heating to 65 °C in between [Fig. 3(b)] shows that the locations and brightnesses of the spots have not changed significantly: the nanobubbles are at the same location, and their size or morphology is the same (see, for example, bubbles denoted by 1 and 2).

For an assessment of these findings, we first analyze Fig. 3(c), in which we show the substrate surface after a second round of liquid exchange at 20 °C. The surface was flushed with ethanol. This made the bubbles as depicted in frames *A* and *B* of Fig. 3 disappear. Then, after the ethanol-water exchange, again bright spots reminiscent of nanobubbles were visible. Their brightness, contrast, and location distribution are comparable to those in Figs. 3(a) and 3(b). Quite remarkably, some bubbles appear again at the same location (denoted by 1). But they also appear at new locations (3), and, occasionally, locations that were occupied with bubbles before now remain bubble-free (2). This means that specific substrate locations do facilitate the nucleation or growth of nanobubbles, but they do not dominate it. These findings endorse important conclusions in evaluating Fig. 3(b). If the amount and/or location of the nanobubbles changed upon heating to 65 °C, this would also show up as a change in the distribution of the nanobubbles after cooling. However, as there is no dominating preference of nanobubbles for specific substrate sites, and as the bubble distribution remains unchanged after the heat treatment, we conclude that the bubbles most likely remain stable and unaltered up to 65 °C [21].

Conclusion.—With nonintrusive interference-enhanced reflection microscopy, we visualized surface nanobubbles and investigated their growth dynamics. Bright spots were identified as individual surface nanobubbles. This could be concluded from the correlation of their appearance with sample preparation protocol and validated by accompanying AFM investigations. We showed that nanobubbles exist without external intrusion and that they appear and fully develop within seconds (or faster) after the replacement of ethanol by water. We could also show that the nanobubbles remain stable and unaltered up to 65 °C. Last but not least, sequential nanobubble preparation revealed that the bubbles sometimes appear at the same spots, and sometimes they do not. Their growth is therefore not dominated by preferred or active surface sites, although there is a certain preference for certain locations. All this was not generally accepted up until now, because the only technique for imaging nanobubbles previously, AFM, is intrusive and its time resolution is much worse. The latter also holds for most of the nonimaging methods for nanobubble investigations. Supposedly, the method introduced here can still be optimized to render it much faster ($\ll$ s) and be employed to investigate the flow of the liquid phase in the vicinity of the bubbles with particle tracking.

H. R., S. K., and E. D. thank Helmuth Möhwald for scientific advice and general support. S. K. was supported by the DFG (RI1529/16-1). D. L., H. Z., J. S., and E. D. acknowledge funding from the Foundation for Fundamental Research on Matter (FOM) and the technology foundation STW, which are sponsored by the Netherlands Organization for Scientific Research (NWO). We further acknowledge Ecole de Physique des Houches, where the concept of this work was engineered during the Nanobubbles@LesHouches workshop, February 2012, as well as Frank Holsteyns.

*Stefan.Karpitschka@mpikg.mpg.de
†E.Dietrich@utwente.nl
‡J.R.T.Seddon@utwente.nl
§H.J.W.Zandvliet@utwente.nl
‖D.Lohse@utwente.nl
¶Hans.Riegler@mpikg.mpg.de

[1] V. S. J. Craig, Soft Matter **7**, 40 (2011).
[2] J. R. T. Seddon and D. Lohse, J. Phys. Condens. Matter **23**, 133001 (2011).
[3] X. H. Zhang, A. Quinn, and W. A. Ducker, Langmuir **24**, 4756 (2008).
[4] H. Seo, M. Yoo, and S. Jeon, Langmuir **23**, 1623 (2007).
[5] X. H. Zhang, Phys. Chem. Chem. Phys. **10**, 6842 (2008).
[6] R. Steitz, T. Gutberlet, T. Hauss, B. Klösgen, R. Krastev, S. Schemmel, A. C. Simonsen, and G. H. Findenegg, Langmuir **19**, 2409 (2003).
[7] D. A. Doshi, E. B. Watkins, J. N. Israelachvili, and J. Majewski, Proc. Natl. Acad. Sci. U.S.A. **102**, 9458 (2005).
[8] M. Mezger, H. Reichert, S. Schöder, J. Okasinski, H. Schröder, H. Dosch, D. Palms, J. Ralston, and V. Honkimäki, Proc. Natl. Acad. Sci. U.S.A. **103**, 18 401 (2006).
[9] N. Ishida, T. Inoue, M. Miyahara, and K. Higashitani, Langmuir **16**, 6377 (2000).
[10] S.-T. Lou, Z.-Q. Ouyang, Y. Zhang, X.-J. Li, J. Hu, M.-Q. Li, and F.-J. Yang, J. Vac. Sci. Technol. B **18**, 2573 (2000).
[11] R. Köhler, P. Lazar, and H. Riegler, Appl. Phys. Lett. **89**, 241906 (2006).
[12] C. C. Chan and C.-D. Ohl, arXiv:1204.2633.
[13] H. Rathgen, Ph.D. thesis, University of Twente, 2008.
[14] We get similar results with perfluorodecyltrichlorosilane.
[15] S. Lou, J. Gao, X. Xiao, X. Li, G. Li, Y. Zhang, M. Li, J. Sun, X. Li, and J. Hu, Mater. Charact. **48**, 211 (2002).
[16] X. H. Zhang, N. Maeda, and V. S. J. Craig, Langmuir **22**, 5025 (2006).
[17] A. C. Simonsen, P. L. Hansen, and B. Klösgen, J. Colloid Interface Sci. **273**, 291 (2004).
[18] B. M. Borkent, H. Schonherr, G. LeCaer, B. Dollet, and D. Lohse, Phys. Rev. E **80**, 036315 (2009).
[19] The left-hand side of the optical distribution is right at the limit of the spatial resolution, as shown with the horizontal

error bar. We again refer to the difficulty to extract the exact nanobubble size from its diffraction pattern.

[20] See Supplemental Material at http://link.aps.org/supplemental/10.1103/PhysRevLett.109.066102 for a comparison of the ethanol-water exchange, and statistics of surface nanobubbles as measured with both AFM and the optical technique.

[21] A direct visualization of the nanobubbles at 65 °C was not possible because of temperature-induced convection and diffractive index variations.